Storm Energy Flux Characterization along the Mediterranean Coast of Andalusia (Spain)

Rosa Molina [1] , Giorgio Manno [2] , Carlo Lo Re [2],* , Giorgio Anfuso [1] and Giuseppe Ciraolo [2]

1   Department of Earth Sciences, Faculty of Marine and Environmental Sciences, University of Cádiz, Polígono del Río San Pedro s/n, 11510 Puerto Real, Spain; r.molina.gil@gmail.com (R.M.); giorgio.anfuso@uca.es (G.A.)
2   Department of Engineering, University of Palermo, Viale delle Scienze, Bd. 8, 90128 Palermo, Italy; giorgio.manno@unipa.it (G.M.); giuseppe.ciraolo@unipa.it (G.C.)
*   Correspondence: carlo.lore@unipa.it; Tel.: +39-238-965-24

check for updates

Abstract: This paper investigates wave climate and storm characteristics along the Mediterranean coast of Andalusia, for the period 1979–2014, by means of the analysis of wave data on four prediction points obtained from the European Centre for Medium-Range Weather Forecasts (ECMWF). Normally, to characterize storms, researchers use the so-called "power index". In this paper, a different approach was adopted based on the assessment of the wave energy flux of each storm, using a robust definition of sea storm. During the investigated period, a total of 2961 storm events were recorded. They were classified by means of their associated energy flux into five classes, from low- (Class I) to high-energetic (Class V). Each point showed a different behavior in terms of energy, number, and duration of storms. Nine stormy years, i.e., years with a high cumulative energy, were recorded in 1980, 1983, 1990, 1992, 1995, 2001, 2008, 2010, and 2013.

Keywords: energy flux; storm classification; stormy year; coastal erosion; Andalusia coast

1. Introduction

Coastal areas are extremely important in Mediterranean countries since they host the majority of their population and economic activities [1]. Over the last few decades, one of the faster urban developments has occurred along the Spanish Mediterranean coast, especially at the Costa del Sol [2]. As a result of this expansion, human activities and buildings were placed extremely close to the shore [3]; therefore, they are now threatened by natural hazards influenced by climate change-related processes such as sea-level rise and increases in storm frequency and intensity [4,5]. To reduce storm impacts, it is necessary to understand specific coastal characteristics and sensibilities as well as to fully comprehend storm nature. In recent years, several researchers have studied these aspects from different viewpoints. In Spain, Rodrıguez-Ramırez et al. [6] studied storm records on the Huelva coast to obtain appropriate future development and management strategies; Mendoza and Jiménez [7] and Mendoza et al. [8] presented an intensity scale for wave storms on the Catalan coast to characterize their spatial and temporal variability; Guisado and Malvárez [9] and Pintado and García [10] used extreme wave conditions to complete the characterization of the morpho-dynamic environments of the Costa del Sol and Huelva areas; Anfuso et al. [11] and [12,13] characterized storms along the Atlantic side of Andalusia. In recent decades, coastal scientists have used several indexes to characterize storms, e.g., Halsey [14] ranked north-east Atlantic coastal storms (northeasters or nor'easters) based on a damage potential index and Dolan and Davis [15] proposed an intensity scale index to classify nor'easters into five classes, from weak to extreme, based on wave height and storm duration. Orford et al. [16] and

Orford and Carter [17] used the role of storm surge to develop a new storm index. Kriebel et al. [18] proposed a nor'easter risk index by combining the effects of storm surge, wave, and duration and Zhang et al. [19] developed a storm erosion potential index by combining the effect of storm tide, wave energy, and duration. This paper analyzes a 35-year wave climate dataset obtained from the European Centre for Medium-Range Weather Forecasts (ECMWF) for four available prediction points equally spaced along the Mediterranean coast of Andalusia (south of Spain). This allowed the definition and assessment of storm characteristics and their spatial and temporal distribution along the investigated area. To characterize the storms, a new approach was adopted, assessing the real wave energy flux of each storm, using a robust definition of the storm itself. During the investigated period, a total of 2961 storm events were recorded. These were classified according to five classes of storms, from low (Class I) to high-energetic (Class V). Results obtained are useful to understand potential impacts of both single and grouped storms, and hence put in place the appropriate prevention and mitigation strategies.

2. The Study Area

This study is focused on the wave climate of the Andalusia Mediterranean coast, a very populated area whose land cover has experienced important changes during recent decades [20]. Málaga is the province that has experienced the most important coastal occupation, in particular due to the construction of structures related to national and international tourism [20]. The coast is a micro-tidal environment (tidal range < 20 cm, [9]), about 546 km long, and including four provinces, i.e., Cádiz, Málaga, Granada, and Almería (Figure 1).
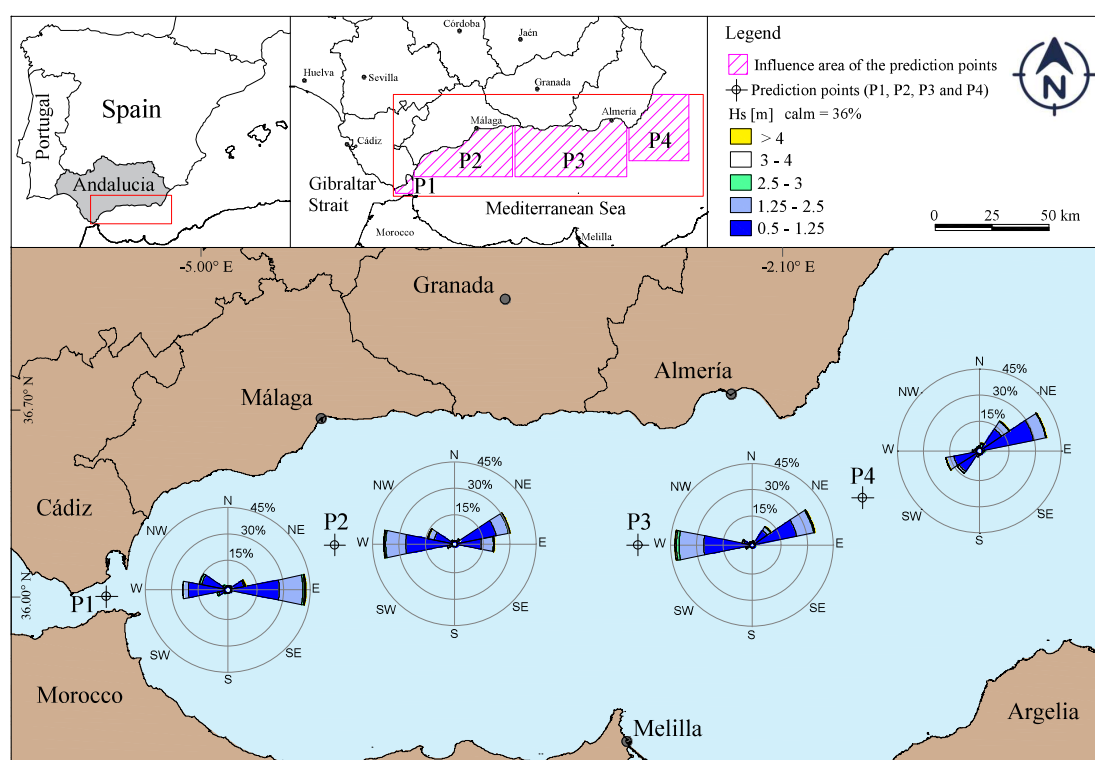

Figure 1. Geographic location of the study area and wave rise (1979–2014) for each prediction point.

There are many Andalusian coastal areas that suffer erosion problems [21], typically linked to very energetic storms producing severe damage to coastal structures. For example, Figure 2 shows the damage produced in winter 2015 by a western storm at Alumuñecar (Granada Province). This storm particularly affected the beaches of San Cristobal and La Herradura. At the former, the extreme wave run-up broke the facilities for summer tourism, and at the latter, storm waves reached the road at several points, depositing cobbles and sand that endangered people the circulation of vehicles.

Figure 2. Severe damage after a western storm in winter 2015 at the Reina Sofia Promenade (Almuñecar), photo by europapress.

On the Mediterranean Andalusian coast, the beaches are rectilinear and composed of medium to fine and dark to golden sands and, especially in Granada and Almería, cliffed sectors are observed. The near-shore area generally shows high slope values and intermediate and reflective morpho-dynamic states linked to a narrow continental shelf [22]. This sector is exposed to winds from E and SE with minimum and maximum wind speed values that range from 0.4 to 0.9 m/s [9].

3. Methods

With the aim of characterizing the wave climate of the studied area, four prediction points were identified along the Mediterranean Andalusian coast; at each point, wave rises and the monthly means of maximum wave height $H_{m0,max}$ were calculated. The wave rises give information about the direction and intensity of incoming waves, whereas the monthly wave height means give information about the seasonal characteristics of the Mediterranean Andalusian coast. To identify each single storm, the definition of [23] was adopted, which allowed calculation of the energy flux by using the linear deep-water wave theory and, finally, classification of energy flux, preferring this parameter to empirical ones.

3.1. Wave Climate Preliminary Analysis

Wave climate analysis was carried out using wave data modelled by the ECMWF by means of the WAve Model (WAM). This numerical model, which solves the energy balance equation, forecasts wave climate that is then subjected to quality controls ensuring its consistency [24] (https://www.ecmwf.int/en/elibrary/16951-wave-model accessed on January 2019). This paper used MATLAB scripts to analyze wave characteristics along the Mediterranean coast of Andalusia for the period 1979–2014, obtained by the ECMWF within the framework of the ERA-INTERIM project. The four predictions points, from W to E, used in this paper, are Point 1, close the Strait of Gibraltar, Point 2, east of Málaga, and Points 3 and 4 in front and east of Almería, respectively (Figure 1). Each temporal series is formed by 51,860 data points recorded over a period of 35 years (1 January 1979–30 January 2014) which is enough to analyze potential trends of increasing wave heights, the presence of climate-controlled cycles, or annual variations due to climate events [5].

3.2. Storm Classification Using the Energy Flux

To determine storm events, the definition used was the one given by [23], i.e., a Mediterranean Sea storm is a sequence of sea states in which the spectrally significant wave height exceeds the

threshold h_t and does not fall below this threshold for a continuous time interval greater than 12 h. He also considered that the time interval between consecutive single storms must be greater than 12 h. The government agency "Puertos del Estado" [25] suggested, for the Mediterranean coast of Andalusia, adopting a threshold value $h_t = 1.5$ m. Boccotti [23] suggests adopting the same value for the threshold (h_t) because it is 1.5 times the mean yearly significant wave height. Following the aforementioned criteria, 2961 storms were selected for the period 1979–2014.

Many studies (e.g., [7,8,11–13]) based the classification of storms on the use of the Dolan and Davis [15] "Storm Power Index". In this paper, a physically based parameter was preferred, namely, wave energy flux [26,27]. Wave energy flux, or wave power per unit of wave-front length (P), was calculated using the following equation:

$$P = \frac{\rho g^2}{64\pi} T_e H_{m_0}^2 \left[\frac{W}{m}\right] \tag{1}$$

where ρ is water density, g is the gravity acceleration, T_e is the energy period that represents the period of the sinusoidal wave with the same energy as a real sea state (for which a JONSWAP spectrum is about 90% of the peak period) and H_{m_0} is the spectrally significant wave height. To obtain an accurate estimation of the total energy (E_{tot}^i) of each storm [26–29] the energy flux was time-integrated:

$$E_{tot}^i = \int_0^{d_i} P dt \left[\frac{Wh}{m}\right] \tag{2}$$

where the d^i is the duration of i-th storm. Using Equations (1) and (2) the total energy of each of the 2961 storms was calculated.

For example, two storms at the prediction Point P3 are shown in Figure 3. The first storm started on 25 February 2009 and the second on 4 March 2009. Figure 3a shows the H_{m0} values of the two storms identified by means of the threshold $h_t = 1.5$ m. The corresponding energy flux P and the total energy E_{tot}^i (Equations (1) and (2)) is shown in Figure 3b.
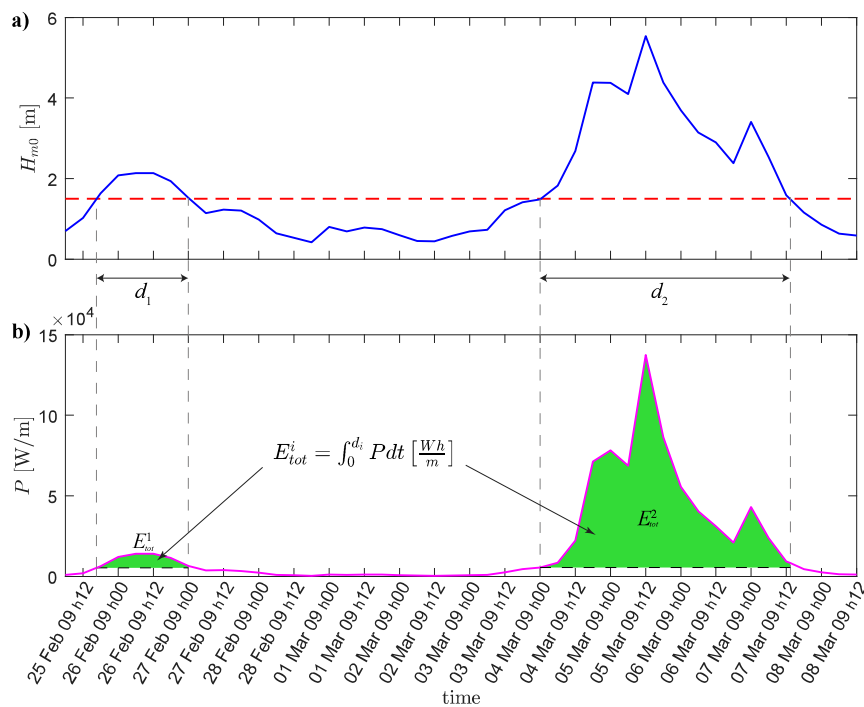

Figure 3. (**a**) Spectrally significant wave height H_{m0}, during the storms of 25 February and 4 March 2009 at the prediction Point P3. The dashed red line is the spectrally significant wave height threshold $h_t = 1.5$ m, d_1 and d_2 are storm duration. (**b**) Energy flux during time and total storm energy.

The method proposed by [30], i.e., "the natural breaks" function, was used to classify storm events into five classes, from Class I (low-energetic events) to Class V (high-energetic events).

The Return Period of the Energy Flux of Storms

For the estimation of the return period of the energy flux (P) of each storm class, the probability of exceedance was fitted with a modification of the Weibull Cumulative Distribution Function (CDF) described in [23,31]:

$$F(P) = e^{-\left(\frac{P}{w}\right)^u} \, [\%] \tag{3}$$

where w and u parameters that depend on the location under examination. Using the auxiliary variables $X = 100 \cdot ln(2.5 \cdot P)$ and $Y = 100 \cdot ln\left[ln\left(1/F(P)\right)\right]$ [23,31], in the coordinate system X, Y, the data points should lie on a straight line. Thus, the parameters of Equation (3) can be easily estimated by fitting those data points by means of the least-squares method.

The above-mentioned Weibull CDF is related to the return period T_r by means of

$$T_r = \frac{1}{\lambda \cdot F(P)} \, [year] \tag{4}$$

where λ is the mean number of events per year. Consequently, for the lower and upper limit of each storm class, the probability of exceedance and the return period were calculated.

3.3. Stormy Year

For the sake of continuity with previous research [11,32], the definition of stormy year was adopted here. In particular, for each prediction point, stormy year empirical recurrence period (R_i) and annual frequency of occurrence (f_o) were assessed by using the equations:

$$R_i = \frac{(n+1)}{m} \, [year] \tag{5}$$

$$f_o = \frac{1}{R_i} \, [\%] \tag{6}$$

where R_i is the recurrence interval calculated for n number of years (35 in this paper), m is the number of events that occurred within the date-range of interest, and f_o is the yearly frequency of occurrence of the event. For each prediction point, two values of R_i and f_o were calculated using a minimum and a maximum threshold, respectively. The minimum threshold is the mean of total energy (μ) calculated within the whole period of 35 years, the maximum threshold is $\mu + \sigma$, where σ is the standard deviation of the total energy.

4. Results and Discussion

4.1. Wave Height Characterization

Wave height data did not present a general trend along the investigated period, but a clear seasonal behavior was recognized, as observed by Rangel-Buitrago and Anfuso [13] on the Atlantic sector of Andalusia. As a general trend, higher average values of monthly maximum spectrally significant wave heights ($H_{m0,max}$) were observed during the winter season, i.e., the December–March period and, specifically, Points 1, 2 and 4 recorded maximum values in March and Point 3 in February (Figure 4). High values recorded in March are linked to the great importance of eastern waves due to regnant winds during such months. Lower average $H_{m0,max}$ values were observed during the summer time, i.e., July, August, and September, ranging from 1.7 m at Point 1 to 2.1 m at Point 3. Dealing with the behavior of each analyzed point, Point 3 showed the highest values in all years, always followed by Point 2; but during June, July, and August, Point 4 recorded greater values than Point 2 (Figure 4).
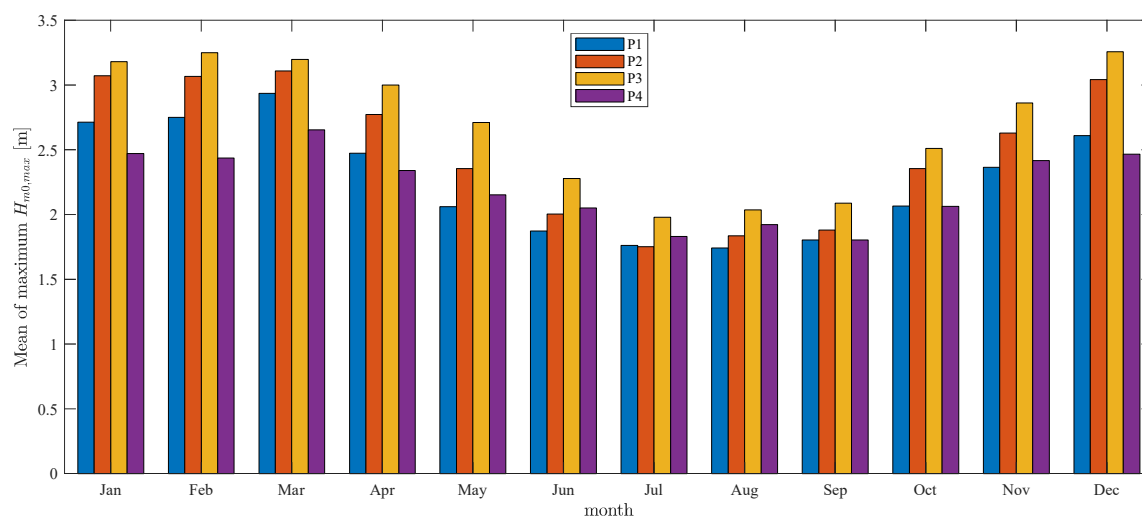
Figure 4. Average values of monthly maximum spectral significant wave heights $H_{m0,max}$.

Approaching directions observed at different points clearly reflected coastal orientation and prevailing marine climate (Figure 1). Point 1 is close to the Strait of Gibraltar but sheltered to the Atlantic swell waves. East approaching fronts, with prevailing wave height classes of 0.5–1.25 m (c. 30%) and 1.25–2.5 (c. 10%), clearly prevailed at this prediction point (Figure 1) and were linked to the strong easterly winds associated with a surface pressure gradient over the Gibraltar Strait when the Azores high pressure is located over the Iberian Peninsula, while there is pronounced low pressure over northern Africa [33]. Points 2 and 3 are situated at the central part of the investigated area, so they are exposed to winds and waves from W and E and E-NE directions; specifically, at Point 2, E and N approaching waves are equivalent to W approaching fronts. At Point 3, the western component prevailed on the north-east approaching direction because of the increase of the western geographic fetch; an increment of the NE component was also observed since this point is more exposed to this approaching direction with respect to Point 2 because of coastal orientation (Figure 1). At Point 4, despite the prevalence of the E-NE approaching direction, the NE component becomes even more evident than at Point 3. Furthermore, since this latter point is sheltered to the west because of coastal orientation (NNE-SSW oriented), waves approaching from the third quadrant essentially present SW and W-SW components.

4.2. Storm Characterization

During the investigated period, a total of 2961 storm events were categorized into five classes, i.e., Class I (weak), Class II (moderate), Class III (significant), Class IV (severe), and Class V (extreme). Points 3 and 2 recorded the highest number of storms (Figure 5). The distribution is similar at all points, with a clear dominance of events belonging to Classes I and II: 87.4% in Point 1, 86.6% in Point 2, 83.1% in Point 3, and 90.4% in Point 4 (Table 1, Figure 5). Mean wave height value of each class did not present great spatial variations, i.e., all points recorded similar values of wave height for the same class. Concerning maximum and minimum wave height values per class, a clear and general trend was not observed, e.g., Point 4 presented the lowest wave height value for Class III but the highest for Classes IV and V (see Table 1).

Table 1. Storm characteristics at each prediction point: class, energy (E_{tot}), frequency of storms, significant wave height (H_{m0}) peak period (T_p), and duration (D).

| Point	Class	E_{tot} [Wh/m]			Frequency [%]	H_{m0} [m]		T_p [s]	D [days]
		Min	Max	Mean		Mean	Standard Deviation	Mean	Mean
1	I	108	503	265	59.6	2.01	0.26	6.5	0.9
	II	503	1100	730	27.8	2.61	0.37	7.4	1.9
	III	1100	2102	1509	8.3	3.27	0.48	8.1	2.9
	IV	2102	4179	2624	3.5	3.64	0.65	8.5	4.2
	V	4179	9165	5635	0.7	4.68	0.98	9.7	4.8
2	I	108	503	272	58.9	2.05	0.29	6.5	0.9
	II	503	1100	749	27.6	2.65	0.38	7.4	2.0
	III	1100	2102	1484	9.9	3.13	0.50	7.9	3.3
	IV	2102	4179	2752	2.3	3.76	0.62	8.6	4.8
	V	4179	9165	5551	0.4	4.73	0.76	9.2	6.9
3	I	108	503	270	55.0	2.05	0.28	6.5	0.9
	II	503	1100	739	28.0	2.69	0.39	7.4	1.9
	III	1100	2102	1460	12.4	3.22	0.47	8.0	3.1
	IV	2102	4179	2775	3.4	3.99	0.52	8.9	4.4
	V	4179	9165	5632	0.9	4.87	0.74	9.5	7.0
4	I	108	503	280	67.1	2.03	0.27	6.8	0.9
	II	503	1100	712	23.2	2.52	0.35	7.6	2.0
	III	1100	2102	1408	8.3	3.12	0.46	8.3	3.0
	IV	2102	4179	2802	0.9	4.34	0.60	9.6	3.3
	V	4179	9165	5248	0.3	5.18	0.49	10.6	3.7
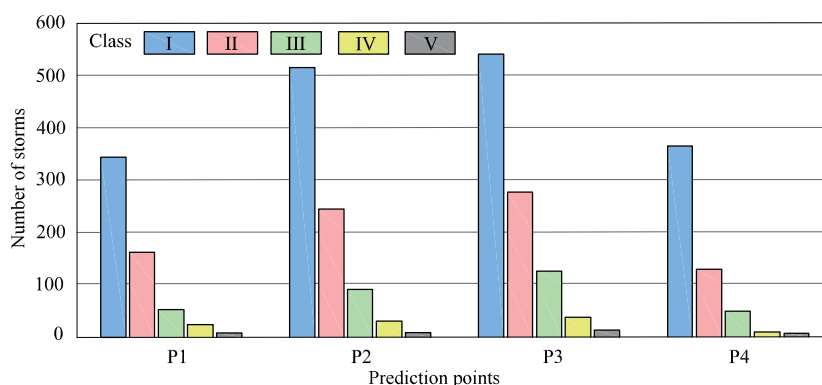
Figure 5. Distribution of storm events per class at each point.

Regarding wave period, the same storm classes of different points presented similar values. Higher wave period variations among classes were recorded at Points 2 and 3 (Table 1). The mean storm duration presented an increase from Class I to Class V at each point (especially Points 2 and 3) and important differences among points (Table 1). Figure 6 reports the monthly distribution of all storms (i.e., the sum of all events recorded at each points) per class. Results are very similar to those obtained by [7,8,11–13,15,34] in their respective studies. Concerning temporal distribution, Classes I and II storms were observed along the whole year. Class III storms were recorded in winter and spring seasons (from October to May), with a minimal occurrence during summer months, i.e., June (8 storms), August (2 storms), and September (2 storms). Class IV storms were observed from November to March, and Class V storms were only recorded from December to March (especially in February, with 7, and March, with 5 events). It is interesting to observe that Classes II and III are very frequent in March, because it relates to approaching waves generated by E and SE winds that are quite frequent in springtime.
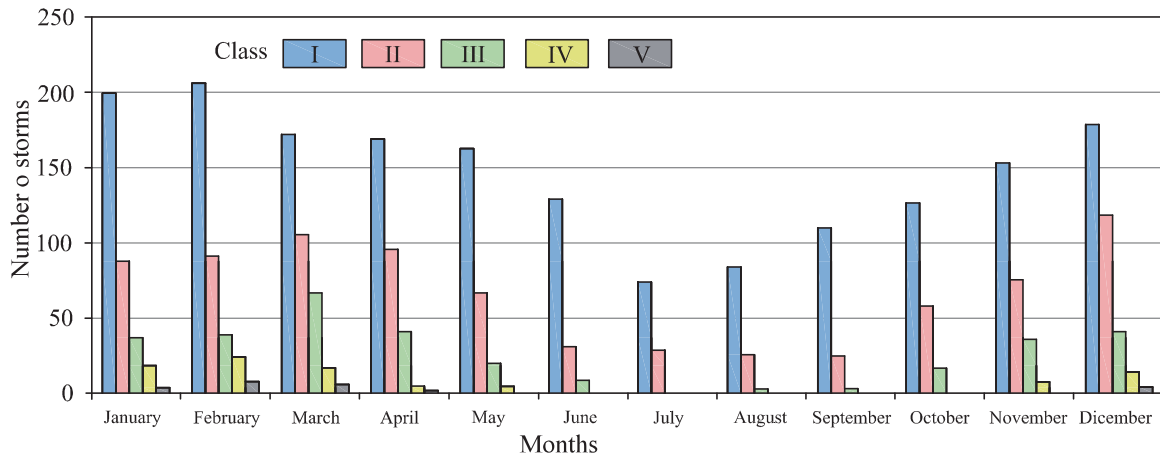
Figure 6. Monthly distribution of all storm events per class and month.

Concerning approaching directions, at Point 1, Classes I and II mainly approached from the east with a small western component (Figure 7) and Classes III, IV and V almost exclusively (>95% of records for each class) approached from E and were linked to the predominant eastern storm waves (Figure 1). At Point 2, the sum of the E and E-NE directions is broadly equivalent to the western component (Figure 7) and clearly reflects, with a slight increase of the eastern component, the wave rise shown in Figure 1. At Point 3, storm energy classes approaching directions (Figure 7) broadly reflect wave rise presented in Figure 1 with an increase of the importance of the western component for all storm classes. At Point 4 (Figure 7), the storm approaching directions are consistent with the wave direction pattern observed in Figure 1. At Point 4, more numerous storms approach from the E-NE direction and disappear in the SW direction. The return period (T_r) of Classes III, IV, and V events at each prediction point are shown in Table 2.
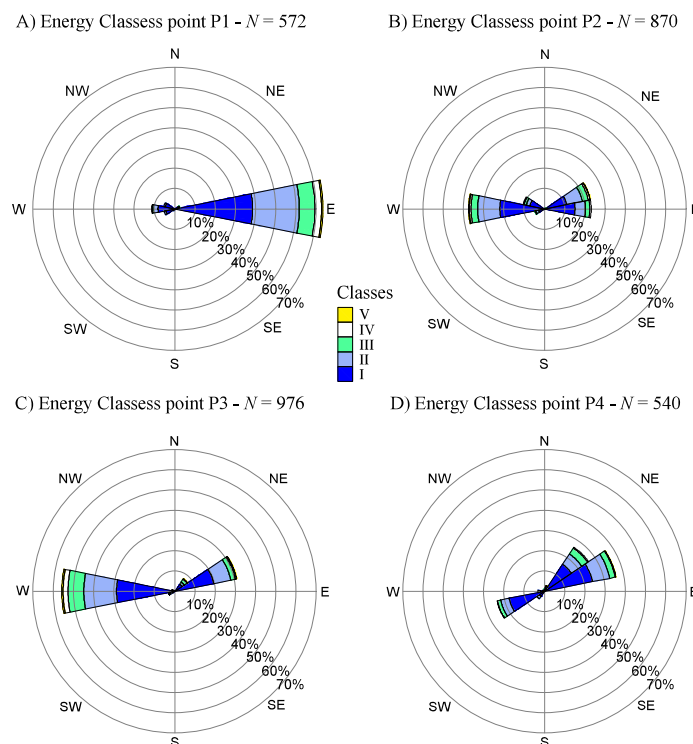

Figure 7. Energy flux roses at all prediction points. (**A**) Point P1, (**B**) Point P2, (**C**) Point P3, (**D**) Point P4. *N* is the total number of storm events.

At Points 2 and 3 the yearly the probability of energy flux exceedance for Class III storms was 100%, varying from 76.9% to 100% at Point 1 and from 43.5% to 100% at Point 4 (Table 2). For Class IV, the probability of occurrence ranged from 41.7% to 100% and from 58.8% to 100% at Points 2 and 3 respectively, and from 27.8% to 76.9% at Point 1 and from 12.7% to 43.5% at Point 4. Class V probability of exceedance have minimum percentages of 12.7% and 18.5% at Points 2 and 3, and 8.4% at Point 1 and 3.3% at Point 4. Mentioned values are broadly similar to observations carried out by Anfuso et al. [11] near the areas of Huelva and Cádiz, i.e., the less energetic zones of Cádiz Gulf. It is observed that the most energetic points (i.e., Points 2 and 3) have the highest percentages of probability of energy flux exceedance (Figure 8), so the facing littoral, i.e., the coast between Málaga and Almería, is very exposed to storms belonging to all classes, and especially to most energetic ones (III, IV, and V) that can have a great impact on both natural and urbanized sectors.
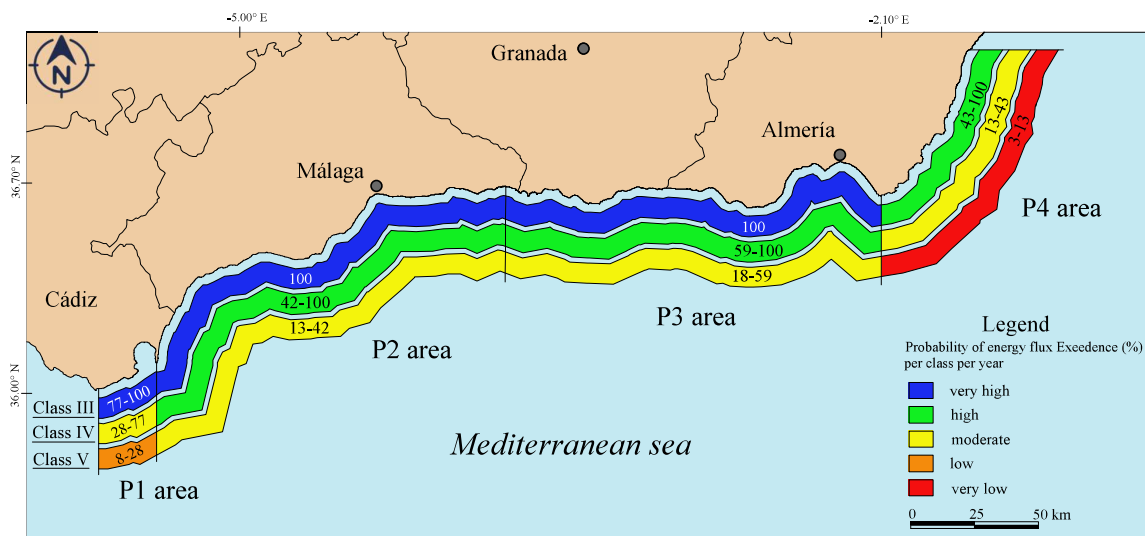

Figure 8. Energy flux probability of exceedance (%) of storms per class III, IV, and V at each point in the coastal area of influence. The percentage values per class as reported on Table 2 are superimposed in the colored stripes.

4.3. Characterization of Stormy Years

In this paper, a special attention was devoted to the yearly cumulative characteristics of storms, i.e., their number, duration, and energy. In fact, as observed by Ferreira [35], the relationship between storms and beach erosion (and/or damage to human structures) varies according to single storm characteristics, storm grouping, and coastal response/morpho-dynamic behavior. Concerning the characterization/quantification of stormy years, only Classes III, IV, and V were considered since these events are the ones that produce important coastal damage according to [12]. With respect to energy data, a similar trend was recorded at the four points, with a similarity observed among Points 1, 2, and 3 (Figure 9).
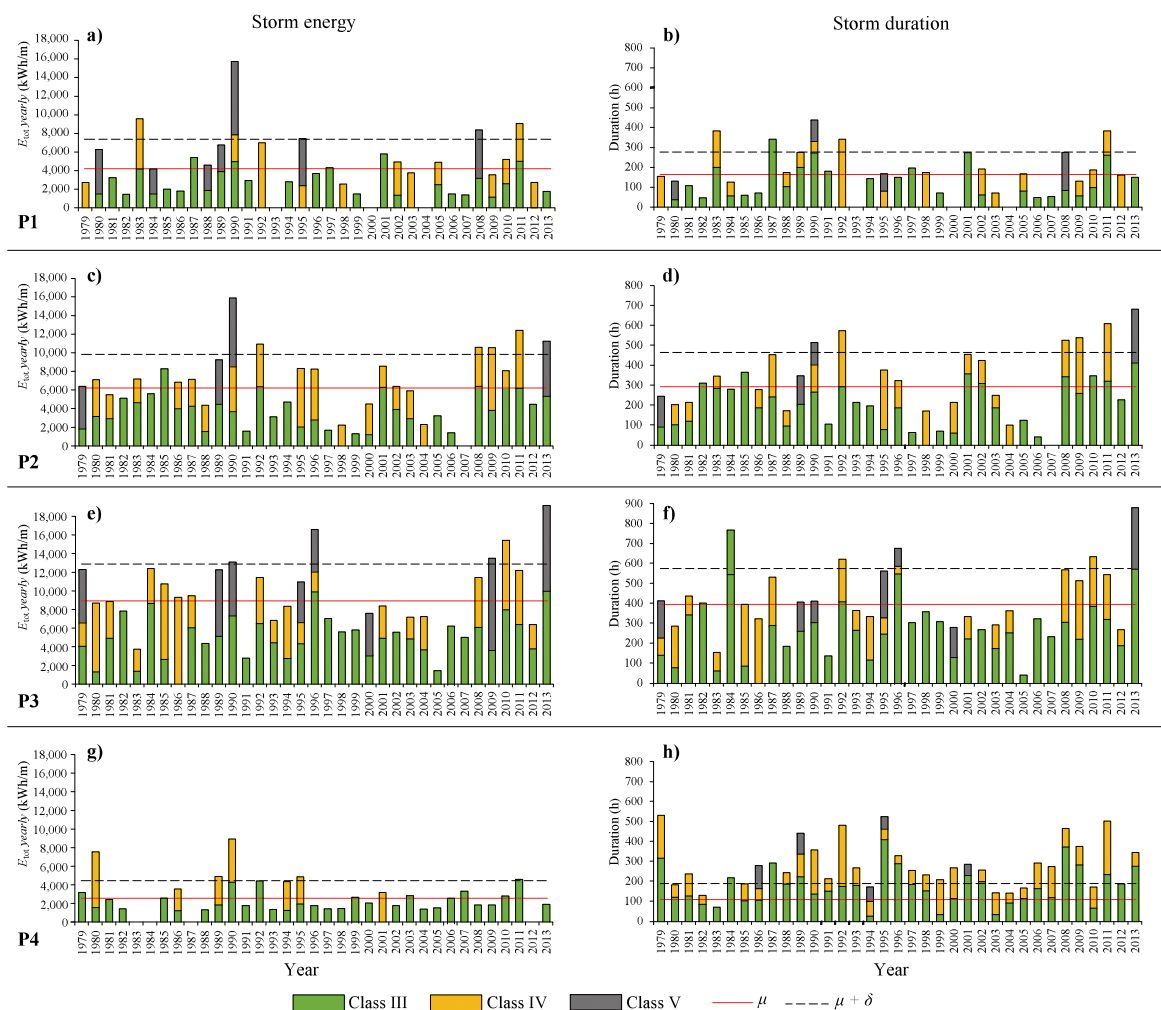
Figure 9. In the left column: the total energy of storms per year for Classes III, IV, and V. At (**a**) Point P1, (**c**) Point P2, (**e**) Point P3, and (**g**) Point P4. In the right column: the corresponding durations of storms (**b**) Point P1, (**d**) Point P2, (**f**) Point P3, and (**h**) Point P4. Red and dashed lines respectively represent the average value (μ) and the average plus one standard deviation ($\mu + \sigma$).

Dealing with yearly energy distribution, it was possible to observe nine energetic years, i.e., 1980, 1983, 1990, 1992, 1995, 2001, 2008, 2010, and 2013. Anomalies were recorded at Point 3, which differed in four of the nine aforementioned years; at Point 1, which recorded a low-energy year in 2013 (i.e., essentially Classes I, II, and III), and at Point 4, which recorded low energy values in 1983, 1984, and 2008 and high values in 1986 and 2007 (Figure 9). Analyzed data of stormy years did not present a clear trend; as an example, yearly distribution of cumulative energy presented a correlation factor (r^2) that ranged from 10^{-5} for Point P2 to 2×10^{-4} for Point P4, but showed a cyclical behavior as highlighted by the calculation of the return period. The recurrence interval and the yearly frequency of occurrence are presented in Table 3 according to the distribution of yearly cumulative energy values (Figure 9). Per each Point, two values of recurrence interval (and frequency of occurrence) are presented, and refer to the mean value and the mean plus one standard deviation of yearly cumulative energy. The frequency of occurrence of stormy year was higher at Point 2 with 17% and 53%, respectively, for the lower and higher energy value, i.e., a low-energetic storm year is observed every 1.9 years and a high-energetic year presents a recurrence interval of 6 years. Point 4 recorded longer recurrence intervals, which ranged from 2.6 to 9 years (39% and 11% values of frequency), respectively, for higher and lower energetic stormy years. Points 1 and 3 presented average values (Table 3).

Table 2. Return period (T_r) and probability of energy flux exceedance ($F(P)$) for the lower and upper limit of each Class (III, IV, V) calculated using Weibull CDF Equation (3). The minimum values are highlighted with blue-colored font.

Point		Class III		Class IV		Class V	
		min	max	min	max	min	max
P1	T_r [year]	<1	1.3	1.3	3.6	3.6	11.9
	$F(P)$ [%]	76.9	100	27.8	76.9	8.4	27.8
P2	T_r	-	<1	<1	2.4	2.4	7.9
	$F(P)$	-	100	41.7	100	12.7	41.7
P3	T_r	-	<1	<1	1.7	1.7	5.4
	$F(P)$	-	100	58.8	100	18.5	58.8
P4	T_r	<1	2.3	2.3	7.9	7.9	30.1
	$F(P)$	43.5	100	12.7	43.5	3.3	12.7

Table 3. Stormy year recurrence interval (R_i) and yearly frequency of occurrence (f_o) calculated from Equation (4), considering yearly cumulative energy values (Figure 9), for each prediction point (Table 1).

Point	Stormy Year			
	R_i [year]		f_o [%]	
	min	max	min	max
P1	2.2	7.2	14	44
P2	1.9	6.0	17	53
P3	2.2	7.2	14	44
P4	2.6	9.0	11	39

Regarding the cumulative storm duration (Figure 9), the trend was not clear. From one side, there is a good correspondence between the number of storms and storm duration within each point, that is, years with many storms also recorded a high cumulative yearly storm duration. Such correspondence was also observed with yearly energy values distribution. On the other hand, no correspondence was observed among different points. A comparison of stormy year distribution recorded in this paper with the one observed by [12] for the Atlantic region of Andalusia showed the opposite behavior linked to the fact that storms on the Atlantic side of Andalusia are essentially related to the predominance of western approaching fronts; meanwhile, on the Mediterranean side [36], they are essentially linked to eastern approaching fronts.

5. Conclusions

To prevent and reduce coastal erosion and damages to human structures, as well as the comprehension of past and future climate trends and beaches' annual and seasonal behavior and evolution, it is very important to characterize the local sea climate. This paper shows as wave climate considerably varies along the Mediterranean coast of Andalusia, from a relatively sheltered area (Point 1) close to the Gibraltar Strait, exclusively affected by easterly wave fronts, to a very energetic central area (Points 2 and 3) exposed to both western and eastern fronts, and to a low-energy area (Point 4) that, because of coastal orientation, is sheltered to western and very exposed to eastern fronts. This behavior is evident when analyzing wave approaching data: main approaching storm directions for high-energy events ranged from E at Point 1, from E to W at Point 2 (only from W for Class V), from W with a small E-NE component at Point 3, and from NE at Point 4 with secondary W-SW components for Classes III and IV (13.33% W for Class III and 20% SW for Class IV). Points 2 and 3 were the most energetic points due to high-energy events approaching from western directions. Stormy years were considered years with a great cumulative energy of Classes III to V events. Nine stormy years were

selected during the investigated period, i.e., 1980, 1983, 1990, 1992, 1995, 2001, 2008, 2010, and 2013. Finally, this study highlighted that the yearly probability of energy flux exceedance of more energetic events is higher in the central sector of the studied area, i.e., at Points 2 and 3, Class III events have a 100% probability; Class IV have a 41.7 to 100% probability; and Class V have a 12.7 to 58.8% probability of energy flux exceedance, so this area has a high sensitivity to storm impacts. Future investigations should be devoted to the analysis of the effects on natural and urbanized coastal environments of single representative storms of each storm class to better understand how an increase in energy and storm duration affects coastal behavior, which is strictly linked to beach morpho-dynamic state, and damages to human structures. Secondly, the effects of storm groupings should be better investigated since erosion and damages to coastal structures greatly depend on cumulative storm energy, on separation between storm events, and on natural beach recovery rates.

Author Contributions: Data curation, R.M., G.M. and C.L.R.; Formal analysis, R.M., G.M. and C.L.R.; Methodology, R.M., G.M., C.L.R., G.A. and G.C.; Software, C.L.R. and G.M.; Supervision, G.A., G.C.; Writing—original draft, R.M., G.M., C.L.R., G.A. and G.C.; Writing—review & editing, C.L.R., G.M., G.A. and G.C.

Conflicts of Interest: The authors declare no conflict of interest.

Abbreviations

The following abbreviations and symbols are used in this manuscript:

CDF	Cumulative Distribution Function
ECMWF	European Centre for Medium-Range Weather Forecasts
ERA-Interim	ECMWF Reanalysis (from January 1979 onward)
POT	Peak Over Threshold
WAM	Wave Model

Symbols

d^i	Duration of i-th storm
E_{tot}^i	Total energy i-th storm
$F(P)$	Weibull Cumulative Distribution Function of energy flux
f_o	Frequency of occurrence related to the empirical recurrence interval
g	Gravity acceleration
H_{m0}	Spectral significant wave height
$H_{m0,max}$	Monthly mean of maximum spectral wave height within the studied date-range (35 years)
h_t	Wave height threshold for storm definition
λ	Mean number of events per year
m	Number of events (upper threshold) within the studied date-range (35 years)
μ	Mean of total energy within the studied date-range (35 years)
N	Number of storm events
P	Energy flux or wave power per unit of wave-front length
R_i	The stormy year empirical recurrence interval
ρ	Water volumetric mass density
σ	Standard deviation of total energy within the studied date-range (35 years)
T_e	Energy period
T_r	Return period related to the probability of exceedance
u	Weibull function second parameter
w	Weibull function first parameter
X	Abscissa of auxiliary variable for linear fitting
Y	Ordinate of auxiliary variable for linear fitting

References

1. Ministerio de Medio Ambiente y Medio Rural y Marino. *Evolución de las Zonas Costeras en Europa*; Editorial Ministerio de Medio Ambiente: Madrid, Spain, 2008; Volume 1, p. 108.
2. Garcia, G.M.; Pollard, J.; Rodriguez, R.D. Origins, management, and measurement of stress on the coast of southern Spain. *Coast. Manag.* **2000**, *28*, 215–234.
3. Manno, G.; Lo Re, C.; Ciraolo, G. Uncertainties in shoreline position analysis: The role of run-up and tide in a gentle slope beach. *Ocean Sci.* **2017**, *13*, 661–671. [CrossRef]
4. Bacon, S.; Carter, D.T. Wave climate changes in the North Atlantic and North Sea. *Int. J. Climatol.* **1991**, *11*, 545–558. [CrossRef]
5. Komar, P.D.; Allan, J.C. Increasing hurricane-generated wave heights along the US east coast and their climate controls. *J. Coast. Res.* **2008**, *24*, 479–488. [CrossRef]
6. Rodrıguez-Ramırez, A.; Ruiz, F.; Cáceres, L.; Vidal, J.R.; Pino, R.; Muñoz, J. Analysis of the recent storm record in the southwestern Spanish coast: Implications for littoral management. *Sci. Total Environ.* **2003**, *303*, 189–201. [CrossRef]
7. Mendoza, E.T.; Jiménez, J.A. Clasificación de tormentas costeras para el litoral catalán (Mediterráneo NO). *Tecnología y Ciencias del Agua* **2008**, *23*, 21–32.
8. Mendoza, E.; Jimenez, J.; Mateo, J.; Salat, J. A coastal storms intensity scale for the Catalan sea (NW Mediterranean). *Nat. Hazards Earth Syst. Sci.* **2011**, *11*, 2453–2462. [CrossRef]
9. Guisado, E., Malvárez, G.C. Multiple scale morphodynamic mapping: methodological considerations and applications for the coastal atlas of Andalusia *J. Coast. Res.* **2009**, *56*, 1513–1517.
10. Pintado, E.G.; García, G.C.M. El estado morfodinámico de las playas a través de modelización numérica de propagación y asomeramiento del oleaje: El frente litoral de Doñana. *GeoFocus. Revista Internacional de Ciencia y Tecnología de la Información Geográfica* **2015**, *1*, 163–180.
11. Anfuso, G.; Rangel-Buitrago, N.; Cortés-Useche, C.; Castillo, B.I.; Gracia, F. Characterization of storm events along the Gulf of Cadiz (eastern central Atlantic Ocean). *Int. J. Climatol.* **2016**, *36*, 3690–3707. [CrossRef]
12. Rangel-Buitrago, N.; Anfuso, G. Coastal storm characterization and morphological impacts on sandy coasts. *Earth Surf. Processes Landf.* **2011**, *36*, 1997–2010. [CrossRef]
13. Rangel-Buitrago, N.; Anfuso, G. Winter wave climate, storms and regional cycles: The SW Spanish Atlantic coast. *Int. J. Climatol.* **2013**, *33*, 2142–2156. [CrossRef]
14. Halsey, S. Proposed classification scale for major northeast storms: East coast, USA based on extent of damage. In *Geological Society of America, Abstracts with Programs (Northeastern Section)*; Geological Society of America: Boulder, CO, USA, 1986; Volume 18, p. 21.
15. Dolan, R.; Davis, R.E. An intensity scale for Atlantic coast northeast storms. *J. Coast. Res.* **1992**, *8*, 840–853.
16. Orford, J.; Hinton, A.; Carter, R.; Jennings, S. A tidal link between sea level rise and coastal response of a gravel-dominated barrier in Nova Scotia. *Geophys. Monogr.* **1992**, *11*, 71–79.
17. Orford, J.; Carter, R. Examination of mesoscale forcing of a swash-aligned, gravel barrier from Nova Scotia. *Mar. Geol.* **1995**, *126*, 201–211. [CrossRef]
18. Kriebel, D.; Dalrymple, R.; Pratt, A.; Sakovich, V. Shoreline risk index for northeasters. In Proceedings of the 1996 Conference on Natural Disaster Reduction, Washington, DC, USA, 3–5 December 1996.
19. Zhang, K.; Douglas, B.; Leatherman, S. Beach erosion potential for severe nor'easters. *J. Coast. Res.* **2001**, *17*, 309–321.
20. Manno, G.; Anfuso, G.; Messina, E.; Williams, A.; Suffo, M.; Liguori, V. Decadal evolution of coastline armouring along the Mediterranean Andalusia littoral (South of Spain). *Ocean Coast. Manag.* **2016**, *124*, 84–99. [CrossRef]
21. Fernandez-Nunez, M.; Díaz-Cuevas, P.; Ojeda, J.; Prieto, A.; Sánchez-Carnero, N. Multipurpose line for mapping coastal information using a data model: The Andalusian coast (Spain). *J. Coast. Conserv.* **2015**, *19*, 461–474. [CrossRef]
22. Guisado, E.; Malvárez, G.C.; Navas, F. Morphodynamic environments of the Costa del Sol, Spain. *J. Coast. Res.* **2013**, *65*, 500–505. [CrossRef]
23. Boccotti, P. *Wave Mechanics for Ocean Engineering*; Elsevier: Amsterdam, The Netherlands, 2000; Volume 64.

24. Dee, D.; Uppala, S.; Simmons, A.; Berrisford, P.; Poli, P.; Kobayashi, S.; Andrae, U.; Balmaseda, M.; Balsamo, G.; Bauer, P.; et al. The ERA-Interim reanalysis: Configuration and performance of the data assimilation system. *Q. J. R. Meteorol. Soc.* **2011**, *137*, 553–597. [CrossRef]

25. Puerto del Estado *Recomendaciones para Obras Marítimas R.O.M. 0.3-91. Oleaje. Anejo I. Clima Marítimo en el Litoral Español*; Technical Report; Ministerio de Obras Públicas y Transportes: Madrid, Spain, 1992.

26. Monteforte, M.; Lo Re, C.; Ferreri, G.B. Wave energy assessment in Sicily (Italy). *Renew. Energy* **2015**, *78*, 276–287. [CrossRef]

27. Lo Re, C.; Manno, G.; Ciraolo, G.; Besio, G. Wave Energy Assessment around the Aegadian Islands (Sicily). *Energies* **2019**, *12*, 333.

28. Iglesias, G.; Carballo, R. Wave energy potential along the Death Coast (Spain). *Energy* **2009**, *34*, 1963–1975. [CrossRef]

29. Vicinanza, D.; Cappietti, L.; Ferrante, V.; Contestabile, P. Estimation of the wave energy in the Italian offshore. *J. Coast. Res.* **2011**, *64*, 613–617.

30. Jenks, G.; Caspall, F. Error on Choroplethic Maps: Definition, Measurement, Reduction. *Ann. Assoc. Am. Geogr.* **1971**, *61*, 217–244. [CrossRef]

31. Lo Re, C.; Cannarozzo, M.; Ferreri, G.B. Present-day use of an empirical wave prediction method. *Proc. Inst. Civ. Eng. Marit. Eng.* **2016**, *169*, 3–14. [CrossRef]

32. Almeida, L.; Vousdoukas, M.; Ferreira, Ó.; Rodrigues, B.; Matias, A. Thresholds for storm impacts on an exposed sandy coastal area in southern Portugal. *Geomorphology* **2012**, *143–144*, 3–12. [CrossRef]

33. Dorman, C.; Beardsley, R.; Limeburner, R. Winds in the strait of gibraltar. *Q. J. R. Meteorol. Soc.* **1995**, *121*, 1903–1921. [CrossRef]

34. Moritz, H.; Moritz, H. Evaluating extreme storm power and potential implications to coastal infrastructure damage, Oregon Coast USA. In Proceedings of the 9th International Workshop on Wave Hindcasting and Forecasting, Victoria, BC, Canada, 24–29 September 2006.

35. Ferreira, Ó. Storm groups versus extreme single storms: Predicted erosion and management consequences. *J. Coast. Res.* **2005**, *42*, 221–227.

36. Menéndez, M.; Mendez, F.J.; Losada, I.J.; Medina, R.; Abascal, A.J. Variaciones del régimen extremal del clima marítimo en el litoral español en el periodo 1958–2001. In *El Clima entre el Mar y la Montaña. Asociación Española de Climatología y Universidad de Cantabria, Santander, Serie A*; García Codron, J.C., Diego Liaño, C.F., De Arróyabe Hernáez, P., Garmendia Pedraja, C., Rasilla Álvarez, D., Eds.; Asociación Española de Climatología (AEC): Santander, Spain, 2004; Volume 4, pp. 73–84.